

The interaction of poly(L-lactic acid) and the nucleating agent *N,N'*-bis(benzoyl) suberic acid dihydrazide

Yan-Hua Cai^{1), 2), *)}, Li-Sha Zhao^{1), 2)}

DOI: dx.doi.org/10.14314/polimery.2015.693

Abstract: Since *N,N'*-bis(benzoyl) suberic acid dihydrazide [NA(S)] acts as a powerful nucleating agent for poly(L-lactic acid) (PLLA), it is necessary to study the nucleation mechanism of NA(S) in the crystallization of PLLA. The interaction between PLLA and NA(S) was investigated by Fourier transform infrared spectroscopy (FT-IR), thermogravimetric analysis (TGA) and temperature-dependent Raman spectroscopy. The results from FT-IR and temperature-dependent Raman spectroscopy showed that a hydrogen bond between the C=O of PLLA and the N-H of NA(S) was formed. The TGA also indicated the existence of an intense interaction between PLLA and NA(S), resulting in the potent nucleation ability of NA(S) for PLLA. Molecular dynamics simulations (MDS) were employed to simulate the interaction of PLLA on the NA(S) surface. The simulation results further confirmed the hydrogen bond between PLLA and NA(S). The MDS study also analyzed the interaction energy between PLLA and NA(S). The MDS results can be used to select the proper nucleating agents and design novel organic nucleating agents.

Keywords: poly(L-lactic acid), nucleating agent, crystallization, nucleation mechanism, molecular dynamics simulation.

Interakcje między poli(kwasem L-mlekowym) a czynnikiem zarodkującym – *N,N'*-bis(benzoilo)dihydrazydem kwasu suberynowego

Streszczenie: Zbadano mechanizm zarodkowania przy użyciu *N,N'*-bis(benzoilo)dihydrazydu kwasu suberynowego [NA(S)] w procesie krystalizacji poli(kwasu L-mlekowego) (PLLA). Interakcje między cząsteczkami PLLA i NA(S) oceniano na podstawie spektroskopii w podczerwieni z transformacją Fouriera, analizy termograwimetrycznej oraz widm Ramana, rejestrowanych w różnej temperaturze. Stwierdzono, że pomiędzy tlenem z grupy C=O w łańcuchu PLLA a wodorem z grupy N-H obecnej w NA(S) tworzą się wiązania wodorowe. Analiza TGA wykazała, że ww. intensywne interakcje są wynikiem dużej zdolności NA(S) do zarodkowania krystalizacji PLLA. Do zbadania oddziaływań na powierzchni NA(S) zastosowano także symulacje metodą dynamiki molekularnej (MDS), które potwierdziły występowanie wiązań wodorowych PLLA/NA(S). Metodą MDS określono też energię interakcji (technika MDS może być wykorzystana przy wyborze środka zarodkującego odpowiedniego dla danego układu).

Słowa kluczowe: poli(kwas L-mlekowy), czynnik zarodkujący, krystalizacja, mechanizm zarodkowania, symulacja metodą dynamiki molekularnej.

PLLA is one of the most common, biodegradable polymers because it has low energy consumption, is a biomass based monomer and is non-toxic to the environment [1]. PLLA represents an interesting alternative route to common, non-degradable polymers for short lifetime applications, such as packaging materials. With the continuous development of PLLA, its applications have

broadened from short-term applications [2–4] to automotive interiors [5, 6] and surgical sutures [7, 8]. What is more, PLLA applications are expected to be carbon neutral from the viewpoint of the reduction of carbon dioxide emission and saving of resources [9]. However, until now, the slow crystallization rate of PLLA has restricted its practical applications. In order to improve the crystallization rate of PLLA, there are four routes that can be used, including minimizing the amount of D-lactide isomers, adding nucleating agents, adding plasticizer and playing with the molding conditions. The most effective method to increase the overall crystallization rate is to blend PLLA with a nucleating agent.

Up to now, many kinds of nucleating agents have been successfully developed to improve the overall crystallization, such as talc [10], montmorillonite [11], layered

¹⁾ Chongqing Key Laboratory of Environmental Materials and Remediation Technologies, Chongqing University of Arts and Sciences, Yongchuan, Chongqing-402160, P. R. China.

²⁾ School of Materials and Chemical Engineering, Chongqing University of Arts and Sciences, Yongchuan, Chongqing-402160, P. R. China.

*) Author for correspondence; e-mail: mci651@163.com

metal phosphonate [12], silica [13], nano calcium carbonate [14], carbon nanotubes [15], ethylene bis(stearamide) [16], inositol [17], benzenetricarboxylamide derivatives [18], etc. These nucleating agents can increase the crystallization rate of PLLA but the nucleation mechanism has been rarely explored. And the nucleation mechanism is very important to investigate the nucleating effect of the additive and design new nucleating agents. There are two proposed nucleating mechanisms between a polymer and a nucleating agent, including the epitaxial nucleation and mechanisms of the chemical reactions [12]. As for epitaxial nucleation, the crystals will epitaxially grow on the surface of the nucleating agent. In this case, the growing of the crystals is governed by the matching of the lattice planes of the polymer and nucleating agent. This mechanism has been widely used to explain the nucleation of polymer/nucleating agents systems such as PET/talc [19], PLLA/zinc phenylphosphonate [12], etc. The chemical nucleation thinks that a chemical reaction between polymer and nucleating agents occurs, resulting in the formation of a new nucleating compound that can induce the nucleation of other polymer chains.

In our previous work [20], *N,N'*-bis(benzoyl) suberic acid dihydrazide [NA(S)] was synthesized for use as a nucleating agent. Upon the addition of 0.8 wt % NA(S), the crystallization half-time of PLLA decreased from 26.5 min to 1.4 min at 115 °C. Why does the NA(S) have an advanced nucleating ability for PLLA? It is well known that the NA(S) improves the crystallization of PLLA. Here, the reason that PLLA/NA(S) had a faster crystallization rate must be the changed structures of PLLA and NA(S). According to the chemical structures of PLLA and NA(S), an interaction is expected to occur between NA(S) and PLLA.

Thus, in this paper, the interaction between PLLA and NA(S) was investigated by Fourier transform infrared spectroscopy (FT-IR), thermogravimetric analysis (TGA) and temperature-dependent Raman spectroscopy. Meantime, molecular dynamics simulations (MDS) were employed to simulate the interaction of PLLA on the NA(S) surface.

EXPERIMENTAL PART

Materials

— Poly(L-lactic acid) ($M_w = 1.95 \cdot 10^5$) was purchased from Nature Works LLC, USA, and the 2002D PLLA has a D content of 4.25 %.

— The other chemical reagents used in this work were of analytical grade (AR). Benzoyl hydrazine and suberic acid were procured from Beijing Chemical Reagents, China and Chengdu Kelong Chemical Reagents, China, respectively. *N,N*-dimethylacetamide, thionyl dichloride and pyridine were procured from Mianyang Rongshen Chemical Reagents Company, China.

Synthesis of *N,N'*-bis(benzoyl) suberic acid dihydrazide

N,N'-bis(benzoyl) suberic acid dihydrazide was synthesized as in our previous work [20].

Preparation of PLLA/NA(S) samples

Similarly, the preparation procedure of PLLA/NA(S) samples was reported in our previous work [20].

Methods of testing

Simulation methods and models

The simulation was carried out with Materials Studio v4.4 software packages commercially available from Accelrys (Available software modules within Accelrys Materials Studio 4.4 include Amorphous Cell, Dmol3, DPD, GULP, MesoDyn, MesoTek, ONESTEP, QMERA, Discover, etc.), and all calculations were performed using an empirical force field since relatively large systems were studied [21]. In this study, the force field was COMPASS. The COMPASS force field is a general, all-atom force field for atomistic simulation, and it enables the accurate prediction of structural, vibration, conformation and physical properties of molecules and condensed phases [22]. Thus, the COMPASS force field has been applied to study the adhesion of copper with an acrylonitrile-butadiene-styrene interface [23]. The simulation was carried out at a temperature of ~25 °C, controlled by the Andersen algorithm, and the equilibration of the structures was performed in the isothermal-isochoric (NTV) canonical ensemble with periodic boundary conditions applied. The duration of the simulations was confined to 50 ps using a time step of 1 fs. The simulation time was confined to 50 ps because, within this time period, the temperature of the system reached its preset value and no changes of the non-bond and potential energy of the systems were observed.

Infrared spectra

Fourier transform infrared spectra of PLLA/NA(S) films were recorded on a Bio-Rad FTS135 spectrophotometer from 4000 to 400 cm⁻¹.

Thermogravimetric analysis

TGA was performed using a Q500 thermal analysis instrument with a heating rate of 20 deg/min under an air flow (60 cm³/min) from room temperature to 500 °C.

Temperature-dependent Raman spectroscopic

The temperature-dependent Raman spectroscopy data was measured on a Renishaw InVia Plus Raman

spectrometer. The Raman spectrum of NA(S) was recorded at room temperature. The Raman spectra of neat PLLA and PLLA/0.8 wt % NA(S) were recorded after isothermal crystallization at 105 °C, 115 °C, 125 °C, 140 °C. In addition, the Raman spectra of the neat PLLA and PLLA/0.8 wt % NA(S) were recorded at room temperature and 160 °C.

RESULTS AND DISCUSSION

FT-IR analysis of the interaction between PLLA and NA(S)

Figure 1 shows the IR spectra of PLLA, NA(S) and PLLA/NA(S) with different NA(S) contents. There is a strong absorption band at 1753.9 cm⁻¹, which is assigned to the carbonyl (C=O) stretching vibration of PLLA. The phenomena of a blue-shift of the C=O becomes clearer with an increase of NA(S), the absorption of the C=O shifts to 1748.5 cm⁻¹. The reason may be that there exists an interaction between the carbonyl group of PLLA and an active group of NA(S), resulting in the charge of the group of C=O moving to other atoms, and the absorption frequency of C=O decreasing. Thus, the absorption of C=O shifts to lower frequency.

increase of NA(S). The reason may be as follows, the absorption of the C=O of PLLA/NA(S) after isothermal crystallization is so strong that the absorption of the adjacent C=O including a hydrogen bond is not observed. In addition, the size of the particles of PLLA/NA(S) are more than 10 microns, which results in more reflection of incident light, thus, the intensity of absorption peaks weakens.

Raman analysis of interactions between PLLA and NA(S)

In order to further investigate the hydrogen bond between PLLA and NA(S), Raman spectroscopy was employed. Figure 2 presents the Raman spectra of PLLA and NA(S) at room temperature. The Raman spectrum of PLLA has been reported in some detail [25, 26]. Bands at 1444.7 cm⁻¹, 1378.2 cm⁻¹ and 1124.5 cm⁻¹ in the micro-Raman spectra of PLLA are assigned to CH₃ asymmetric deformation vibrations, symmetric deformation vibrations and asymmetric rocking vibrations, respectively. The bands for PLLA observed at 1760.4 cm⁻¹ and 732.6 cm⁻¹ are assigned to C=O stretching vibrations and in-plane deformation vibrations. The absorption peak at 1292.6 cm⁻¹ contributes to the absorption of C-H deforma-

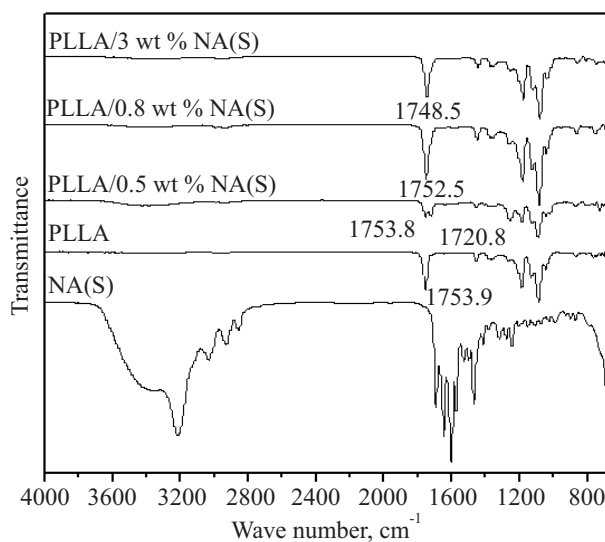


Fig. 1. IR spectra of PLLA, NA(S) and PLLA/NA(S) after isothermal crystallization

In addition, upon the addition of 0.5 % NA(S), the stretching vibration of C=O splits into two absorption peaks compared to the carbonyl peak of pure PLLA. One peak at 1753.8 cm⁻¹ is assigned to the original C=O vibration of PLLA. Another peak appears at 1720.8 cm⁻¹, which is ascribed to the interaction of PLLA and NA(S). This result is coincident with the results reported by Zhou [24]. However, it is also observed that the stretching vibration of C=O does not split into two absorption peaks with an

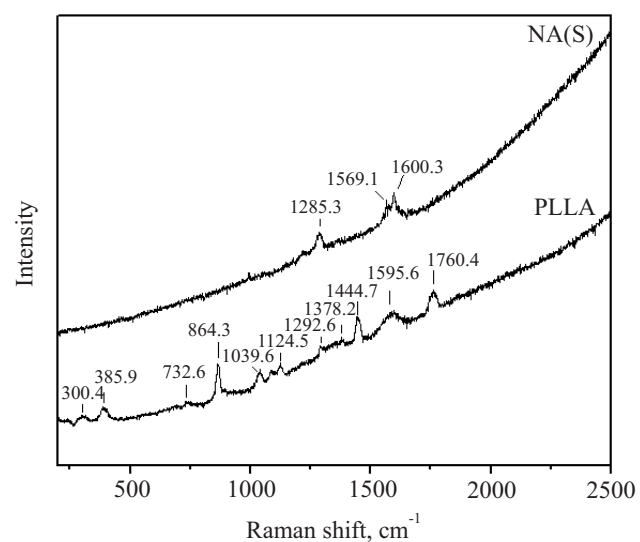


Fig. 2. Raman spectra of PLLA and NA(S) at room temperature

tion vibration, and the absorption peaks at 1039.6 cm⁻¹ and 864.3 cm⁻¹ belong to C-CH₃ and C-COO stretching vibrations, respectively. A band at 385.9 cm⁻¹ for PLLA is assigned to COO deformation vibrations, and the absorption at 300.4 cm⁻¹ is due to a coupling mode of COC and C-CH₃ deformation vibrations. Compared to neat PLLA, there exist fewer absorption peaks in the Raman spectrum of NA(S), which is due to a more polar group. A band at 1600.3 cm⁻¹ of NA(S) is assigned to the C=O stretching vibration, the absorption peak at 1569.1 cm⁻¹

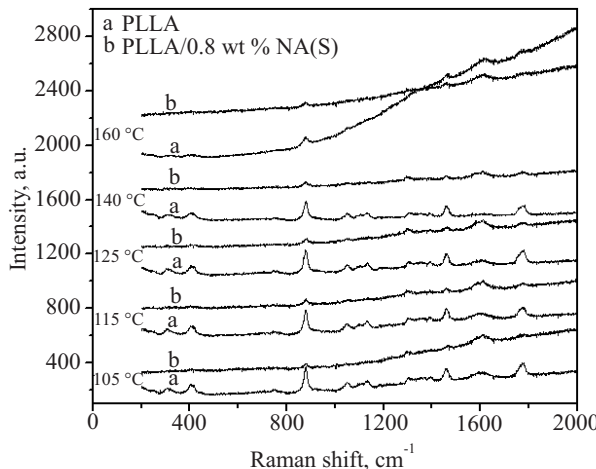


Fig. 3. Raman spectra of PLLA and PLLA/0.8 wt % NA(S) at different temperatures

belongs to C-C of the benzene stretching vibration, and the peak at 1285.3 cm^{-1} belongs to the C-N stretching vibration.

Table 1. Absorption in the Raman spectra of C=O and C-COO in PLLA and PLLA/0.8 wt % NA(S) samples at different temperatures

$T, ^\circ\text{C}$	PLLA		PLLA/0.8 wt % NA(S)	
	C=O (cm^{-1})	C-COO (cm^{-1})	C=O (cm^{-1})	C-COO (cm^{-1})
105	1774.1	880.4	1779.9	880.4
115	1779.1	878.7	1776.6	879.5
125	1779.9	878.7	1776.6	883.8
140	1783.4	880.4	1774.1	881.2
160	1768.1	878.7	1741.9	877.1

Figure 3 shows the Raman spectra of PLLA and PLLA/0.8 wt % NA(S) at different isothermal crystallization temperatures. The absorption of the C=O and C-COO groups of PLLA and PLLA/NA(S) are listed in Table 1. Compared to C=O of the neat PLLA, the absorption peak of C=O of PLLA/NA(S) undergoes a blue-shift at all temperatures higher than 105 °C. This is due to the interaction between N-H of NA(S) and C=O of PLLA, that is to say, there exists a hydrogen bond between N-H and C=O. Similar results can be found in the system of dimethyl sulfoxide and water [27]. What is more, the absorption of C=O weakens after the addition of NA(S), the reason may be that perfection of spherulite of PLLA with NA(S) decreases, and the spherulite has lower crystallinity. In addition, because there exists a hydrogen bond between C=O and N-H, the influence of the oxygen atom on C-C decreases, and the stretching vibration of C-COO strengthens. Compared to the neat PLLA, the stretching vibration of C-COO of PLLA/0.8 wt % NA(S) with the best nucleating effect for PLLA [20] shifts to a higher frequency for 105 °C to 140 °C. However, the stretching vibration of C-COO of PLLA/0.8 wt % NA(S) shifts in the low frequency direction at 160 °C. The reason is that

PLLA is melted at 160 °C, and there exists no interaction between NA(S) and PLLA, which results in the influence of oxygen atom to C-C. These results further confirm that there exist interactions between PLLA and NA(S).

TGA analysis of interaction between PLLA and NA(S)

Thermogravimetric analysis (TGA) curves of the thermal decomposition of pure PLLA and PLLA with different NA(S) contents at heating rates of 20 deg/min are presented in Fig. 4.

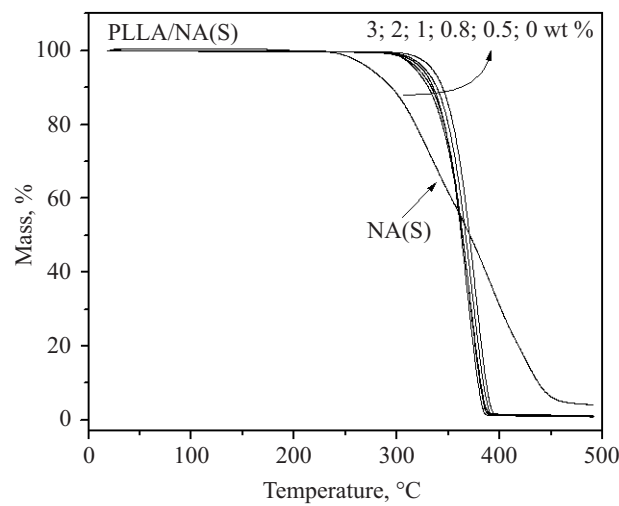


Fig. 4. TGA curves of PLLA, NA(S) and PLLA/NA(S) with various amounts of NA(S)

There exists one stage of decomposition, which indicates the main decomposition products of PLLA. The onset temperature of decomposition of the neat PLLA is 351.48 °C. The TGA curves of PLLA/NA(S) samples are similar to that of the neat PLLA, however, the onset decomposition temperature of PLLA/0.5 wt % NA(S), PLLA/0.8 wt % NA(S), PLLA/1 wt % NA(S), PLLA/2 wt % NA(S) and PLLA/3 wt % NA(S) are 351 °C, 346 °C, 344 °C, 343 °C and 342 °C, respectively. For NA(S), there exists two stages of decomposition during the heating process, and the onset temperature of NA(S) is 285 °C, which indicates that the decomposition temperature of NA(S) increases after addition of PLLA, resulting from the interaction between PLLA and NA(S). As aforementioned, the hydrogen bond between N-H of NA(S) and C=O of PLLA forms, and this force is very intense. When PLLA/NA(S) is heated to decomposition, NA(S) can decompose after the destruction of this bond [28], which results in an increase of the decomposition temperature of NA(S).

Analysis of molecular dynamics simulations of PLLA chains

Figure 5 shows optimized PLLA chains using DMol3, and bonding length and bonding angles were obtained.

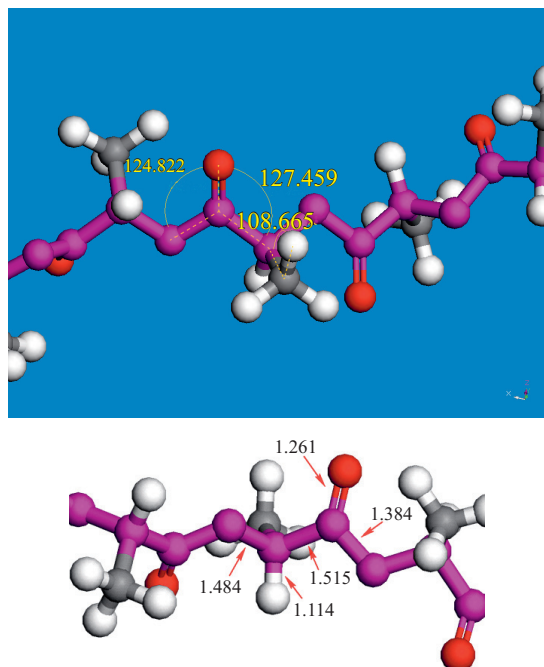
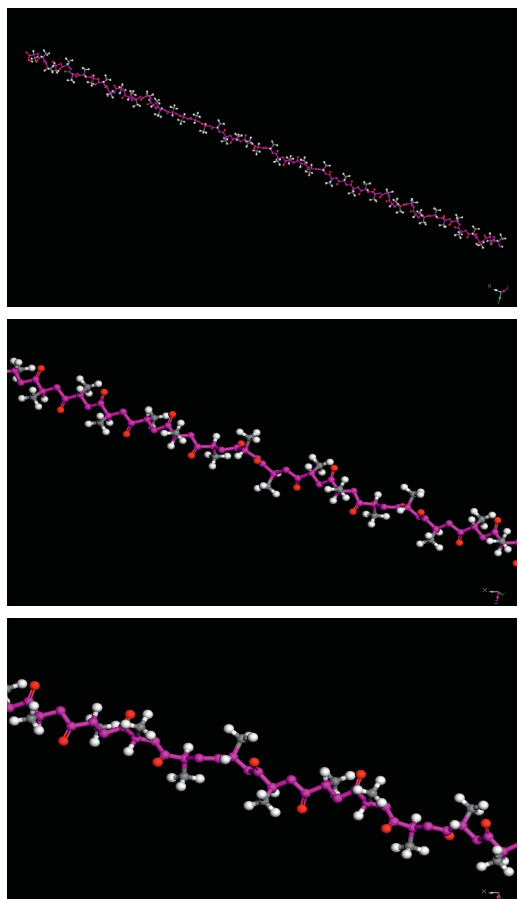


Fig. 6. Bond lengths and bond angles of optimized PLLA

Fig. 5. Patterns of the optimized geometric structure of PLLA

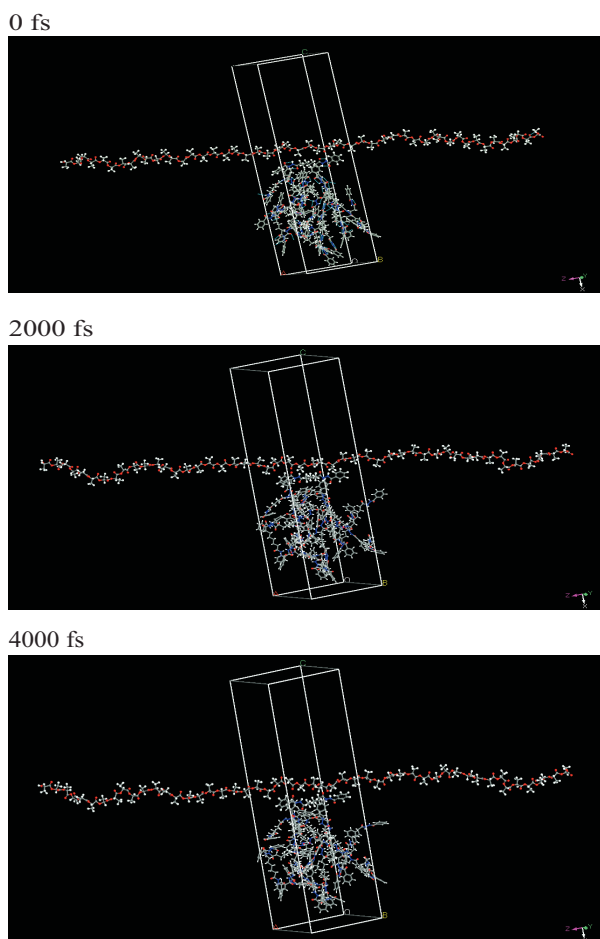


Fig. 7. Simulation process of PLLA/NA(S) using Discover

As shown in Fig. 6, the bond lengths and angles among atoms of PLLA are consistent with the literature [29, 30], which indicates that simulation using DMol3 is accurate. On the other hand, the C=O and α carbon of C-H of PLLA chains is not in a side, and there exists no hydrogen bond between C=O and α carbon of C-H.

Interaction energy between PLLA and NA(S)

Figure 7 shows the system of PLLA and NA(S) at different simulation times. It is found that NA(S) is constantly close to PLLA chains to achieve equilibrium during increased simulation times. Meantime, the form of PLLA chains also undergoes distortions during the initial simulation stages. The result further indicates that there exists an intense interaction between PLLA and NA(S). What is more, a hydrogen bond is found between C=O groups of PLLA and the N-H groups of NA(S) after the system achieved equilibrium (Fig. 8). That is to say, the hydrogen bond between the C=O in PLLA and N-H in NA(S) played a significant role in the interaction between PLLA and NA(S). The simulation results are consistent with the above experimental results.

The energy of $E_{\text{NA(S)}}$, E_{PLLA} and $E_{\text{PLLA/NA(S)}}$ were obtained by the MDS, and ΔE the energy binding between PLLA

and NA(S) was calculated through the following equation:

$$\Delta E = E_{\text{PLLA/NA(S)}} - (E_{\text{NA(S)}} + E_{\text{PLLA}}) \quad (1)$$

where: $E_{\text{NA(S)}}$ — the energy of the NA(S), E_{PLLA} — the energies of the PLLA chains, $E_{\text{PLLA/NA(S)}}$ — the energy of the NA(S) with PLLA on it, the corresponding energy are 13.68 MJ/mol [PLLA/NA(S)], 6.74 MJ/mol [NA(S)] and 7.44 MJ/mol (PLLA). Note that ΔE is negative (-0.5 MJ/mol), which indicates that there exists a low binding energy and more stable state between PLLA and NA(S).

CONCLUSIONS

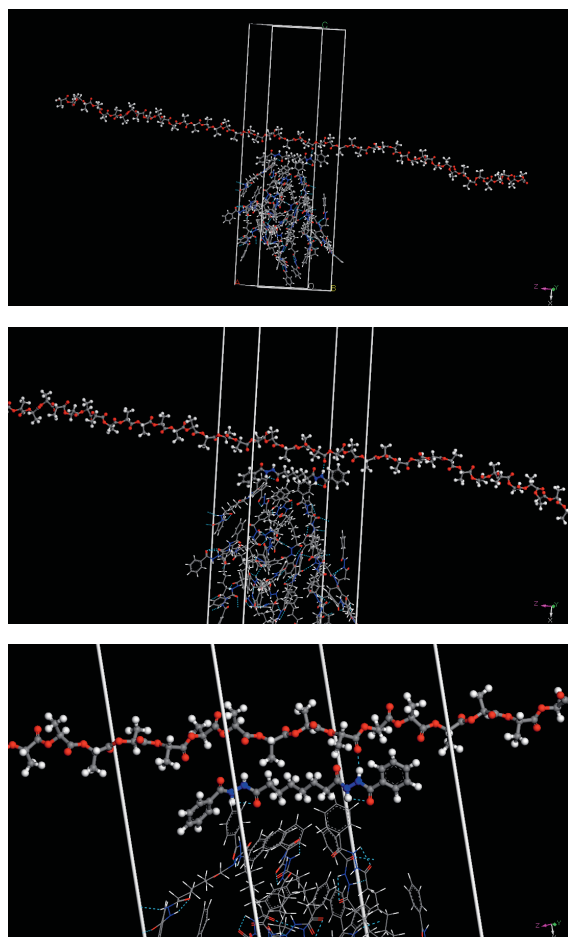
The nucleation mechanism between PLLA and NA(S) was investigated by FT-IR, TGA and temperature-dependent Raman spectroscopic. The results showed that the hydrogen bonds between the C=O of PLLA and the N-H of NA(S) were formed indeed, resulting in the advanced nucleation ability of NA(S) for PLLA. MDS were used to simulate the interaction of PLLA on the NA(S) surface. The hydrogen bonds between PLLA and NA(S) were further analyzed and confirmed by simulation results, this study also obtained the interaction energy between the PLLA and NA(S). The MDS obtained some good results, more in-depth nucleation mechanism of NA(S) will be conducted to verify these results in a future study.

This work was supported by National Natural Science Foundation of China (project number 51403027), China Postdoctoral Science Foundation (project number 2013M531937), Natural Science Foundation Project of CQ CSTC (project number cstc2012jjA50001), Scientific and Technological Research Program of Chongqing Municipal Education Commission (project number KJ131202) and Chongqing University of Arts and Sciences (project number R2013CH11).

REFERENCES

- [1] Tuominen J., Kylma J., Kapanen A. *et al.*: *Biomacromolecules* **2002**, 3, 445. <http://dx.doi.org/10.1021/bm0101522>
- [2] Viljanmaa M., Sodergard A., Tormala P.: *International Journal of Adhesion and Adhesives* **2002**, 22, 219. [http://dx.doi.org/10.1016/S0143-7496\(01\)00057-4](http://dx.doi.org/10.1016/S0143-7496(01)00057-4)
- [3] Viljanmaa M., Sodergard A., Tormala P.: *International Journal of Adhesion and Adhesives* **2002**, 22, 447. [http://dx.doi.org/10.1016/S0143-7496\(02\)00027-1](http://dx.doi.org/10.1016/S0143-7496(02)00027-1)
- [4] Viljanmaa M., Sodergard A., Tormala P.: *Polymer Degradation and Stability* **2002**, 78, 269. [http://dx.doi.org/10.1016/S0141-3910\(02\)00171-4](http://dx.doi.org/10.1016/S0141-3910(02)00171-4)
- [5] Guo W.J., Bao F.C., Wang Z.: *China Wood Industry* **2008**, 22, 12.
- [6] *China pat.* CN101177523A (2008).
- [7] Makela P., Pohjonen T., Tormala P. *et al.*: *Biomaterials* **2002**, 23, 2587. [http://dx.doi.org/10.1016/S0142-9612\(01\)00396-9](http://dx.doi.org/10.1016/S0142-9612(01)00396-9)

Fig. 8. System of PLLA and NA(S) after simulation equilibrium



- [8] Keskin D.S., Tezcaner A., Korkusuz P. *et al.*: *Biomaterials* **2005**, *26*, 4023.
<http://dx.doi.org/10.1016/j.biomaterials.2004.09.063>
- [9] Kawamoto N., Sakai A., Horikoshi T. *et al.*: *Journal of Applied Polymer Science* **2007**, *103*, 198.
<http://dx.doi.org/10.1002/app.25109>
- [10] Ke T.Y., Sun X.Z.: *Journal of Applied Polymer Science* **2003**, *89*, 1203. <http://dx.doi.org/10.1002/app.12162>
- [11] Li X.X., Yin J.B., Yu Z.Y. *et al.*: *Polymer Composites* **2009**, *30*, 1338. <http://dx.doi.org/10.1002/pc.20721>
- [12] Pan P.J., Liang Z.C., Cao A., Inoue Y.: *ACS Applied Materials and Interfaces* **2009**, *1*, 402.
<http://dx.doi.org/10.1021/am800106f>
- [13] Yan S.F., Yin J.B., Yang Y. *et al.*: *Polymer* **2007**, *48*, 1688.
<http://dx.doi.org/10.1016/j.polymer.2007.01.037>
- [14] Liao R.G., Yang B., Yu W., Zhou C.X.: *Journal of Applied Polymer Science* **2007**, *104*, 310.
<http://dx.doi.org/10.1002/app.25733>
- [15] Zhao Y.Y., Qiu Z.B., Yang W.T.: *Composites Science and Technology* **2009**, *69*, 627.
<http://dx.doi.org/10.1016/j.compscitech.2008.12.008>
- [16] Harris A.M., Lee E.C.: *Journal of Applied Polymer Science* **2008**, *107*, 2246. <http://dx.doi.org/10.1002/app.27261>
- [17] Tachibana Y., Maeda T., Ito O. *et al.*: *Polymer Degradation and Stability* **2010**, *95*, 1321.
<http://dx.doi.org/10.1016/j.polymdegradstab.2010.02.007>
- [18] Nakajima H., Takahashi M., Kimura Y.: *Macromolecular Materials and Engineering* **2010**, *295*, 460.
<http://dx.doi.org/10.1002/mame.200900353>
- [19] Haubruege H.G., Daussin R., Jonas A.M., Legras R.: *Macromolecules* **2003**, *36*, 4452.
<http://dx.doi.org/10.1021/ma0341723>
- [20] Cai Y.H., Yan S.F., Yin J.B., Fan Y.Q., Chen X.S.: *Journal of Applied Polymer Science* **2011**, *121*, 1408.
<http://dx.doi.org/10.1002/app.33633>
- [21] Soldera A.: *Polymer* **2002**, *43*, 4269.
[http://dx.doi.org/10.1016/S0032-3861\(02\)00240-9](http://dx.doi.org/10.1016/S0032-3861(02)00240-9)
- [22] Zhang H.P., Lu X., Leng Y. *et al.*: *Acta Biomaterialia* **2009**, *5*, 1169. <http://dx.doi.org/10.1016/j.actbio.2008.11.014>
- [23] Kisin S., Vukic J.B., van der Varst P.G.T. *et al.*: *Chemistry of Materials* **2007**, *19*, 903.
<http://dx.doi.org/10.1021/cm0621702>
- [24] Zhou S.B., Zheng X.T., Yu X.J. *et al.*: *Chemistry of Materials* **2007**, *19*, 247. <http://dx.doi.org/10.1021/cm0619398>
- [25] Kister G., Cassanas G., Vert M.: *Polymer* **1998**, *39*, 267.
[http://dx.doi.org/10.1016/S0032-3861\(97\)00229-2](http://dx.doi.org/10.1016/S0032-3861(97)00229-2)
- [26] Kister G., Cassanas G., Vert M. *et al.*: *Journal Raman Spectroscopy* **1995**, *26*, 307.
<http://dx.doi.org/10.1002/jrs.1250260409>
- [27] Ouyang S.L., Zhou M., Cao B. *et al.*: *Chemical Journal of Chinese Universities* **2008**, *29*, 2055.
- [28] Liao Y.Z., Xin M.H., Li M.C.: *Chemical Industry and Engineering Progress* **2007**, *26*, 725.
- [29] Aleman C., Lotz B., Puiggali J.: *Macromolecules* **2001**, *34*, 4795. <http://dx.doi.org/10.1021/ma001630o>
- [30] Hoogsteen W., Postema A.R., Pennings A.J. *et al.*: *Macromolecules* **1990**, *23*, 634.
<http://dx.doi.org/10.1021/ma00204a041>

Received 19 V 2014.